ROTATIONAL AND VIBRATIONAL RAMAN SPECTROSCOPY FOR FLOW FROM AN UNDEREXPANDED JET NOZZLE

A Senior Scholars Thesis

by

ALEXANDER CHRISTIAN BAYEH

Submitted to the Office of Undergraduate Research of
of Texas A&M University
in partial fulfillment of the requirements for the designation as

UNDERGRADUATE RESEARCH SCHOLAR

April 2008

Major Subject: Aerospace Engineering

ROTATIONAL AND VIBRATIONAL RAMAN SPECTROSCOPY FOR FLOW FROM AN UNDEREXPANDED JET NOZZLE

A Senior Scholars Thesis

by

ALEXANDER CHRISTIAN BAYEH

Submitted to the Office of Undergraduate Research
Texas A&M University
in partial fulfillment of the requirements for the designation as

UNDERGRADUATE RESEARCH SCHOLAR

Approved by:

Research Advisor: Adonios N. Karpetis
Associate Dean for Undergraduate Research: Robert C. Webb

April 2008

Major: Aerospace Engineering

ABSTRACT

Rotational and Vibrational Raman Spectroscopy for Flow from an Underexpanded Jet Nozzle (April 2008)

Alexander Christian Bayeh
Department of Aerospace Engineering
Texas A&M University

Research Advisor: Dr. Adonios Karpetis
Department of Aerospace Engineering

The objective of this work is the construction of a fully functioning Raman line imaging spectrometer; and the measurement of pressure, temperature, and chemical concentration in supersonic flows issuing from a jet nozzle. The measurements will be carried out using roational-vibrational Raman line imaging through the axis of the jet exhaust. In this way measurements of the flow field under high pressure, temperature, and velocity can be made without disrupting it. Because of the increasing push for better fuel efficiencies in modern propulsion devices, it is essential to examine the flow fields within these devices more closely. The high pressure and temperature, even supersonic, environments that are within these modern day devices are simulated by examining the properties of Mach disks in the exhaust of an underexpanded nozzle. Benefits of this research can be applied to turbojets, ramjets, afterburners, and rockets to increase efficiency and overall thrust. Laser techniques have often been used in the past to measured temperature at a known constant pressure or were able to collect both but for only one type of molecule. The technique being used offers pressure, temperature, and

chemical makeup measurements for a non uniform flow field for all the different molecules. Very few labs in the world can perform these types of measurements, and such a lab is currently being assembled on campus. The result of the research at hand is a lab facility with a Raman spectrometer and laser optical system capable of collection spectral data, and an initial investigation into the properties of Mach disks.

TABLE OF CONTENTS

Page

LIST OF FIGURES

CHAPTER I

INTRODUCTION

This research aims to measure the thermodynamic properties of exhaust from an underexpanded jet nozzle using laser diagnostics. More specifically, the areas of interest within the exhaust are the Mach disks caused by expansions and shocks in the exhaust. Mach disks are regions of high temperature and pressure in the flow that are also supersonic. In the exhaust of a jet or rocket engine, these regions tend to be pressures and temperature that are high enough to cause unburned fuel in the flow to ignite[1]. The motivation for this project is the problem of combustion timescales within a supersonic combustion chamber. In a supersonic combustion chamber, the incoming air and fuel have passed through the nozzle before the process of combustion is complete. A better understanding of supersonic combustion can be obtained through the study of combustion within Mach disks. The timescales of supersonic combustion can be studied by analyzing the thermodynamic properties such as temperature, pressure, and species concentration within the Mach and disk along the jet axis.

A major component of this research is the design and construction of a rotational-vibrational Raman spectrometer. The combination of rotational and vibrational Raman

---

This thesis follows the style of the *AIAA Journal*.

spectroscopy is a new technique that will be possible to utilize because of recent advances in optics technology, more specifically high pass optics filters. The implementation of this filter blocks out the Rayleigh scattering signal, which would otherwise the charge-coupled device (CCD) camera from picking up the rotational and vibrational Raman scattering signals. This is very crucial to the design and construction of the spectrometer, because Raman signals are approximately 1000 weaker than Rayleigh signals. Once a spectrum is captured by the CCD camera, species concentrations can be calculated using the signal strengths of the various vibrational Raman signals for difference molecules. Using the species concentration data a temperature can be calculated numerically using the roational Raman signal, and pressure can be calculated using both the calculated species concentrations and temperatures. This spectroscopy system is a new method which offers line measurements, rather than point measurements, and only requires one CCD camera that can obtain all the data for various molecules. One of the biggest benefits of using laser spectroscopy to obtain these measurements is that it is a non-intrusive method. Traditional probes for measuring pressure and temperature are not introduced into the flow and subsequently altering it. This is especially true in supersonic flows where introducing a probe into the flow would induce shock wave, and give rise to incorrect data.

Past experimental research in the area of Mach disks, has been done using Coherent Anti-Stokes Raman Spectroscopy (CARS)[2.] The problem with the CARS laser

technique, however, is that its measurements only work for one pre-selected species, typically N_2. Using the CARS technique, numerous lasers and spectrometers would have to be setup, each for a different species, to attempt to come close to what Raman spectroscopy can do. Systems employing both Raman and Rayleigh scattering techniques have been utilized in previous research to obtain line measurements of turbulent flames[3,4]. This system requires at least two CCD cameras because of the same reason that a high pass filter is introduced into the current spectrometer; the Rayleigh scattering signal is approximately 1000 times greater than the Raman signal, and would wash it out.

CHAPTER II

OVERVIEW OF MACH DISKS

As a fluid element passes the throat of a de Laval nozzle, it begins to expand and accelerate, causing the pressure along the axis of the nozzle to decrease. A nozzle is underexpanded if the pressure at the exit is greater than that of the surrounding atmosphere, and contrary to that a nozzle is overexpanded if the nozzle continues to expand the flow such that the exit at the pressure is less than that of the surrounding atmosphere. Once the flow from an underexpanded jet leaves the nozzle, the pressure of the flow has to come into equilibrium with the surrounding atmosphere. In order to do so it expands to the atmospheric pressure through an expansion fan. The expansion waves from the tip of the nozzle, for axisymmetric flow, are reflect off of the centerline, and continue in a path that cause them to reflect off the free jet boundary as compression waves. The free jet boundary is a constant pressure slip line that encompasses the flow of the jet exhaust. After the expansion waves reflect off of the free jet boundary they are compression waves which then come together at a point to form an oblique shock wave[5].

Since axisymmetric flow is assumed for nozzle flow, the oblique shock wave, formed by the reflected compression waves, would then presumably reflect off of the center line of the flow. What actually happens in this condition is the formation of a Mach reflection prior to intersection with the centerline, which produces a shock triple point in the flow field as seen in Fig. 1. The first shock in the triple point is the incoming oblique shock

wave. The second shock is a Mach reflection which is normal to the centerline. This Mach reflection is what forms the Mach disk for axisymmetric flow. For flow that is not axisymmetric, this Mach reflection would also be referred to as a Mach stem. The third shock from the triple point is an oblique shock that is then reflected back off of the constant pressure free jet boundary as an expansion fan[1].

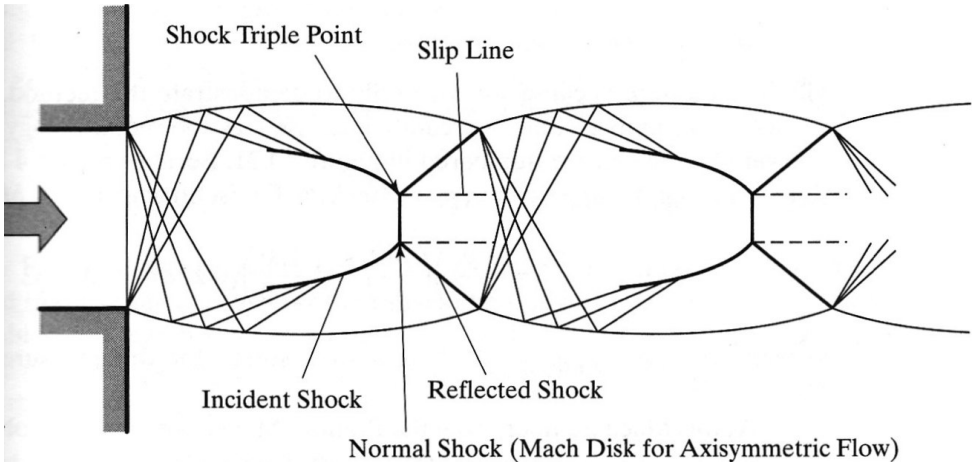

Figure 1. Mach disk formation diagram[1].

The third shock from the shock triple point, the oblique shock, is reflected off of the constant pressure free jet boundary as an expansion wave train would then correspond to the beginning of the process described above. Ideally this process would continue to infinitely occur, but does not because of isentropic losses due to shocks, and viscous effects of the fluid flow. As flow passes through the normal shock (which is also the Mach disk when the shock is rotated about the centerline of the flow), the temperature

and pressure of the flow are elevated. For a hot flow, this elevation in temperature and pressure can cause an ignition of excess fuel in the exhaust[1]. An example of this can be seen in Fig. 2, where the mach disks in the exhaust of the SR-71 Blackbird's engine ignite the excess unburned fuel.

Figure 2. Mach disk ignition from the afterburner of a Lockheed-Martin SR-71 Blackbird[6].

CHAPTER III

THEORY OF RAMAN SPECTROSCOPY

Raman spectroscopy works with two modes of excitation for a molecule. The first mode is the vibrational mode, and the other is the rotational. We will start off first by examining the vibrational modes of a molecule. In examining the vibrational modes of a molecule, an assumption will be made that the diatomic molecule being worked with contains a bond represented as a spring, as a simplification. This simplification is known as the classical harmonic oscillator and has a potential energy curve that is proportional to a quadratic and centered on the unstretched length of the spring, l_e. As the interatomic separation distance l decreases and approaches zero, the classical oscillator does not hold. The interatomic forces between two atoms as they approach each other go to infinity, which corresponds to a potential energy that also diverges to infinity. This is reflected in Fig. 3, which gives an illustration of the Morse potential. The other end of the Morse potential also does not act as a parabolic curve. Instead, as the distance between the two atoms increases, there reaches a point at which they are far enough apart that they are flying away from each other at an almost constant energy. This is represented on the Morse potential by leveling out at an energy level known at the dissociation energy for that molecule[7].

Because of quantum mechanics however, the molecules cannot exist at any point on the Morse potential. Discrete vibrational states, v, at certain energy levels exist that the

molecules must follow, as seen in Fig. 4. Each of these vibrational states has a probability curve that expresses the likelihood of where molecules lie on it. These probability distributions are the solutions to Schrödinger's equation[7]. As there are different vibrational states for a molecule, there are also multiple electronic states, as seen in Fig. 5. These electronic states are represented by multiple Morse potentials at higher energy levels that the molecules can transition to. The amount to excite the molecule to these higher electronic states is much more than the amount of energy to transition the molecule into a different vibrational state.

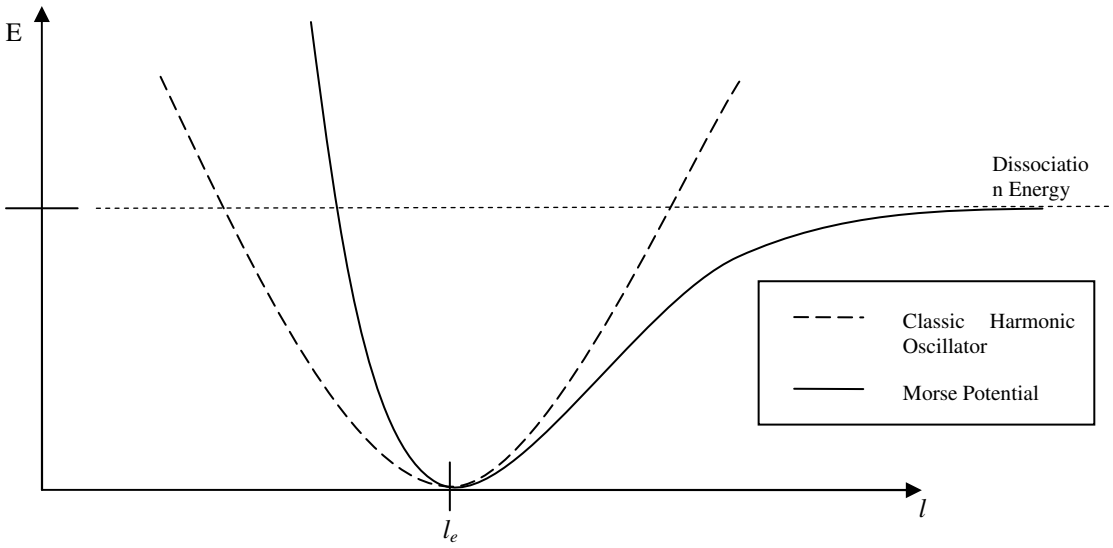

Figure 3. Illustration of the Morse Potential and the Classical Harmonic Oscillator.

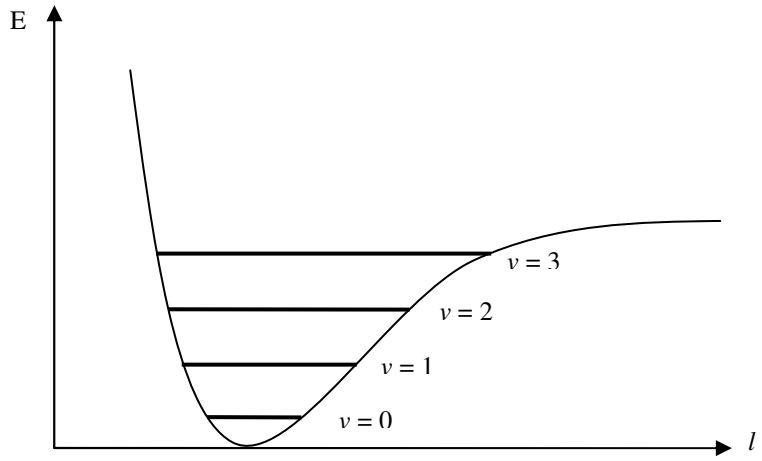

Figure 4. Illustration of the different vibrational states, *v*.

During electronic transitions the atoms in the molecule do not change position, and these transitions are shown on the energy diagram (Fig. 3) by a vertical line between the electronic manifolds. The transition between vibrational states during the electronic transition is mostly determined by the best overlapping between the probability curves of each vibrational state; this is known as the Franck-Condon Principle[7].

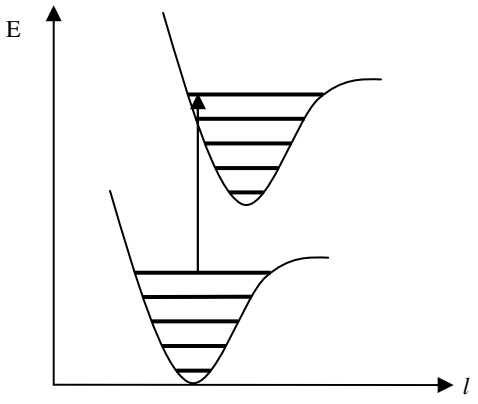

Figure 5. Illustration of multiple electronic states.

Molecules are excited to higher energy level through the process of absorption, and are de-excited through the process of emission. With Raman and Rayleigh scattering, photons are absorbed by the molecules, thus exciting them to a virtual level. A virtual level is an energy level higher than the electronic manifold occupied by the molecule, but less than the next. Virtual levels are not allowed by nature, and thus the molecule must release its energy in the form of a photon. The polarization of the photon released is the same of the original photon that was absorbed. For photons, the equations are:

$$c = \lambda \nu \tag{1}$$

$$E = h\nu \tag{2}$$

where c is the celebrated speed of light, λ is the wavelength of the photon, ν is the frequency of the photon for this equation, E is its energy, and h is Planck's constant.

Rayleigh scattering occurs when the molecule releases a photon that has the same energy as the photon that it absorbed. Because these photons have the same energy, this means that they also have the same frequency and wavelength. This is known as an elastic process because there is no exchange of energy. Raman scattering is, however, an inelastic process; the energy of the emitted photon is different than that of the one than is absorbed. For vibrational Raman scattering, the difference between the energies of the photon emitted and the absorbed photon is due to the molecule being de-excited to a difference vibrational state than where is was prior to excitation[7].

For an absorption and emission process of a molecule that yields an ending vibrational state greater than its initial one, this corresponds to the photon losing energy. Examining Eq. 2, this loss in energy means that the frequency of the emitted photon must also decrease. This decreased frequency leads to an increased wavelength according to Eq. 1, which corresponds to the photon being "red shifted" according to the electromagnetic spectrum. This type of scattering is also known as Stokes Raman scattering. For the opposite situation where the ending vibrational state of a molecule is less than that of its initial, this is known as Anti-Stokes Raman[7] scattering as seen in Fig. 6. The same Stokes and Anti-Stokes shift can also occur for rotational transitions as well. There can be purely vibrational transitions, purely rotational transitions, and a combination of rotational and vibrational transitions by molecule. For each vibrational manifold, there exists a rotational manifold that is superimposed on top of it

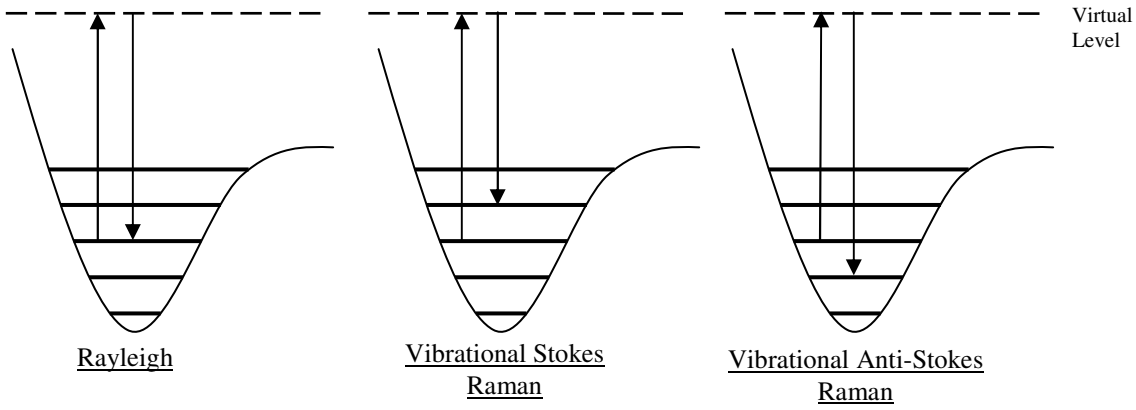

Figure 6. Diagram comparing Rayleigh and Raman scattering.

Pure vibrational Raman is known as vibrational Q-branch Raman. This means that there are no changes in rotational states, also known as O and S- branch Raman. O-branch Raman corresponds to Anti-Stokes Raman, and contrary to that, S-branch Raman corresponds to Stokes Raman. Using pure vibrational Raman species measurements can be made. Once rotational Raman spectra are obtained, temperature measurements can be calculated from the shape of the spectra, and density measurements can be made from a combination of the measured temperature, species concentrations, and the ideal gas equation[7].

The vibrational population N_v is calculated using the following equation,

$$N_v = Ne^{-vhc\omega_e / kT}(1 - e^{-hc\omega_e / kT}) \tag{3}$$

where N is the total number count, v is the vibrational state, ω_e is the molecular vibration frequency, k is Boltzmann's constant, and T is temperature. By dividing the vibrational population by the total number count, a relative vibrational population density can be obtained. The spectral line locations for the various vibrational Stokes transitions $\bar{\nu}$ can be calculated using

$$\bar{\nu}_{v+1,J:v,J} = \bar{\nu}_0 - \left[\omega_e - \omega_e x_e (v+1) - \alpha_e J(J+1)\right] \tag{4}$$

for the vibrational state v, rotational state J, the incident light frequency $\bar{\nu}_0$, the vibrational anharmonicity $\omega_e x_e$, and α_e the vibration-rotation interaction constant[7].

Using the obtained spectra and by examining the strengths of the Stokes vibrational transitions for its different molecules, their species measurements can be made. The signal strength for each species S_{Raman} is given through the relation

$$S_{Raman} = nlP_i\Omega\left(\frac{\partial\sigma}{\partial\Omega}\right)\varepsilon \tag{5}$$

where n is the number density of the selected species, l here is the length of the probe volume, P_i is the power of the incoming laser beam, the solid angle of the collection unit is Ω, $(\partial\sigma/\partial\Omega)$ is the differential scattering cross section of the species, and ε is the efficiency factor of the spectrometer. In order to calculate the molar fraction of each species in the spectra, the sum of the counts of all the Stokes vibrational transitions for the spectra's different species must first be calculated. Then, to obtain each individual species' molar fraction, the individual species' count is then divided by the sum of the counts of all the species for the spectra. Temperature measurements are then made by comparing numerically simulated spectra to the rotational spectra that are captured. Once the temperature and number density measurements are complete, a form of the ideal gas law can be used in order to calculate the partial pressure of each species.

CHAPTER IV

EXPERIMENTAL APPARATUS

An idealized schematic of the multi-scalar Raman measurement system constructed in the lab can be seen in Fig. 7: a pulsed laser beam is focused through the experiment (such as the Mach disks) and the inelastic Raman light collected and imaged onto a spectrometer slit. The light is diffracted through the spectrometer grating and ultimately refocused onto the charge-coupled device (CCD) camera. In this manner one 'image' of the laser is reproduced onto the CCD for every Raman-scattering species present, and is centered along the corresponding vibrational Raman wavelength. Pixel-binning on the CCD is used to increase the number of photons collected for every super-pixel. The size of the super-pixel defines the resolution of the system along the laser axis and along the wavelength axis. The resolution must be adequate enough to resolve the turbulent length scales in physical space and the individual major species in the Raman spectrum. At the same time, and for a given laser power, the overall signal-to-noise (S/N) ratio of the Raman technique increases with super-pixel size, due to the larger number of Raman photons that are collected[7]. Both vibrational and rotational Raman photons are collected onto the same CCD.

Species concentration measurements are done by comparing the relative intensities of species given their rotational scattering cross-sections. Temperature measurements of the flow are then done by comparing the collected rotational Raman spectra to computer

generated spectra for the measured species concentration, and for varying temperatures. Once the measured spectrum is matched to a generated spectrum and the temperature is then specified, pressure can be calculated using the ideal gas law. These measurements are then done for each pixel position along the axis of the laser.

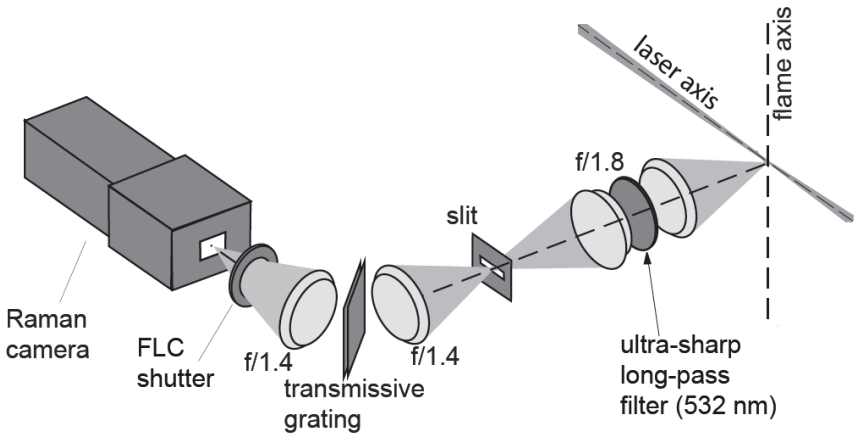

Figure 7. Diagram of the multi-scalar Raman spectroscopy system.

The spectrometer is assembled on an aluminum optics plate in order to make the system capable of being positioned as needed. The first optic placed on the plate is an f/1.8 85 mm lens on top of an optics post. All optics after this point are mounted at the same height using optics posts. An identical lens is placed approximately 15 cm away to focus the light back down from the collimated region. Between these two lenses, in the collimated region, an ultra sharp long-pass filter targeted at 532 nm (the wavelength of the laser) is inserted. It is placed on an optical post, which was mounted on top of a fine adjustable swiveling base that is demarcated in degrees. This is in order to be able to

rotate the filter, as to increase its effectiveness as a long pass filter. At the focal point of the second 85 mm lens, a horizontal slit is placed there in order to block out any ambient light passing through the optics. An f/1.4 50 mm lens is then placed such that its focal point is at the slit, and the light coming through the other side of the lens is collimated.

The next piece of optics to be mounted is the ferroelectric liquid crystal shutter. It is simply placed such that its face was perpendicular to the collimated region and that the light from the collimated region was completely encompassed by the shutter. At this point calculations were made that indicated that the collimated light needed to hit the transmissive grating at an incident angle of 21.1 degrees. It was also calculated that the light exiting the grating would leave at an angle of 21.1 degrees relative to the normal vector of the transmissive grating. In order to mount the grating in this fashion, a fine adjustable swiveling base that is demarcated in degrees is mounted vertically on top of an optical post. From there the transmissive grating is mounted from this swivel and set at an angle approximately equal to 21.1 degrees, and such that the exiting light was directed upwards from the optical plate. Once at this point, a 50 mm lens is attached to the CCD camera used for gathering the spectra and is mounted on a smaller aluminum optical plate. This plate is placed on swiveling brackets, angled at approximately 42.2 degrees, and is raised up on optical posts such that the lens on the CCD camera was aligned with the collimated light exiting the transmissive grating. Figure 8 shows an image of the assembled spectrometer on its optics plate.

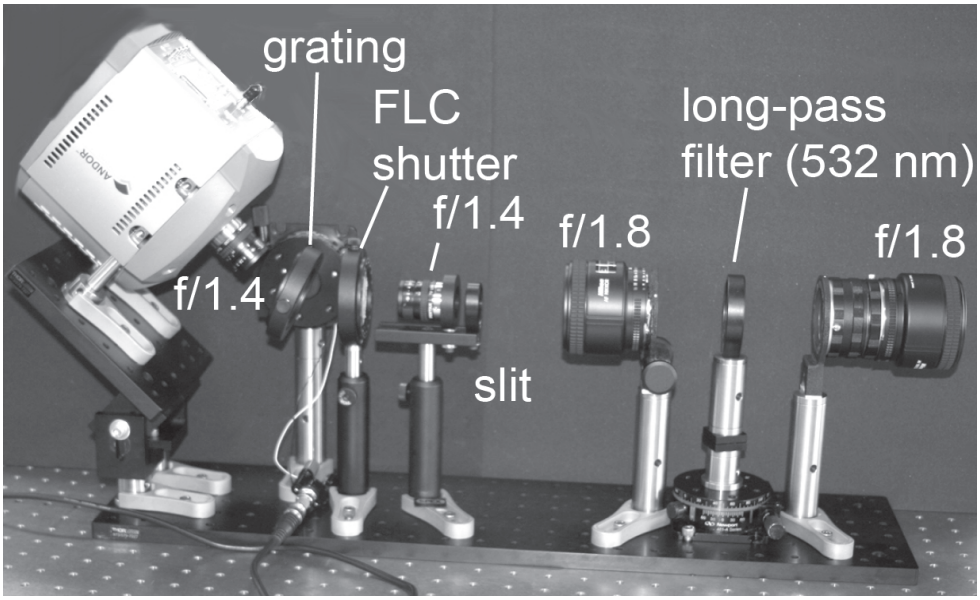

Figure 8. The Raman spectrometer set up in the lab on an aluminum optics plate.

CHAPTER V

SUMMARY

Up to this point in time, only preliminary spectra for calibrations have been collected. The spectrometer is capable of imaging the laser probe volume and collecting spectra, but there is still much more work that has to be done with the spectrometer in order to properly calculate temperature, pressure, and species concentrations for the test section. With the limited amount of time this academic year, and the obligations of undergraduate coursework, fully completing the research in the allotted time was an unfeasible task. However, this research will continue as it will be my project that I will continue in graduate school. In addition, much work needs to be done regarding setting up an underexpanded nozzle with a combustion chamber as a test subjected for the Raman spectrometer.

REFERENCES

[1]John, K., *Gas Dynamics*, 3rd ed., Pearson Education Inc., Upper Saddle River, NJ, 2006.

[2]Kuehner, J. P., Dutton, J. C., and Lucht, R.P., "High-resolution N2 CARS measurements of pressure, temperature, and density using a modeless dye laser." AIAA 2002-2915, 2002

[3]Karpetis, A.N. and Barlow, R.S. Measurements of flame orientation and scalar dissipation in turbulent partially premixed methane flames. *Proceedings of the Combustion Institute*, 30(1), 8, 2004.

[4]Karpetis, A.N., Settersten, T.B., Schefer, R.W. and Barlow, R.S. "Laser imaging system for determination of three-dimensional scalar gradients in turbulent flames." *Optics Letters*, 2004, 29(4), 3.

[5]Chauvet, N., Deck, S., and Jacquin, L., "Shock patterns in a slightly underexpanded sonic jet controlled by radial injections," *Physics of Fluids*, Vol. 19, 2007 Article No. 048104.

[6]Scott, J., "Shock Diamonds and Mach Disks," *AerospaceWeb*, URL: http://aerospaceweb.org/question/propulsion/q0224.shtml [accessed 17 March 2008].

[7]Eckbreth, A.C. *Laser Diagnostics for Combustion Temperature and Species*, 2nd ed, Abacus Press, Cambridge, MA, 1988.

CONTACT INFORMATION

Name:	Alexander Christian Bayeh
Address:	Richardson Building, Rm. 1001, Ross Street College Station TX 77843-3141
E-mail Address:	Abayeh@tamu.edu
Education:	B.S., Aerospace Engineering, Texas A&M University, 2008